

## Numerical Determination of the Magnetic Field Line Hamiltonian

G. KUO-PETRAVIC AND A. H. BOOZER\*

*Plasma Physics Laboratory, Princeton University,  
P.O. Box 541, Princeton, New Jersey 08544*

Received February 12, 1986

The structure of a magnetic field is determined by a one-degree-of-freedom, time-dependent Hamiltonian. This Hamiltonian is evaluated for a given field in a perturbed action-angle form. The location and the size of magnetic islands in the given field are determined from Hamiltonian perturbation theory and from an ordinary Poincaré plot of the field line trajectories. © 1987 Academic Press, Inc.

### I. INTRODUCTION

As early as 1951; Spitzer [1] appreciated that plasma confinement in a torus depends critically on whether the magnetic field lines lie in surfaces, so-called magnetic surfaces, for many transits of the torus. Kerst [2] used an analogy between field lines and particle trajectories to show that a small perturbation could cause magnetic field lines to stray far from simple toroidal surfaces. Rosenbluth *et al.* [3] estimated the rate at which field lines leave a torus if they do not lie in surfaces. Grad [4] has discussed some of the subtleties of toroidal equilibria that are associated with the existence of magnetic surfaces. Even in a given vacuum magnetic field, the determination of the quality of magnetic surfaces is nontrivial. The standard method uses puncture, or Poincaré, plots which require long and numerous field line integrations. Also, the Poincaré plot method of determining surface quality is difficult to automate and to quantify.

This paper implements a Hamiltonian procedure for evaluating the magnetic surface quality of a given magnetic field. A magnetic field is equivalent to a one-degree-of-freedom, time-dependent Hamiltonian system [5]. That is, the three ordinary spatial coordinates can be considered to be functions of the canonical momentum, coordinate, and time of a Hamiltonian with the trajectories of the Hamiltonian being the trajectories of the magnetic field lines. If the magnetic field has a nonzero toroidal component in the spatial region of interest, then the transformation equations between the canonical coordinates and ordinary spatial coordinates are well-behaved, invertible functions. Such transformations preserve structural, or topological, properties; so the Hamiltonian function contains full information on the existence of magnetic surfaces, islands, and stochastic regions.

\* Present address: Dept. of Physics, College of William and Mary, Williamsburg, VA 23185.

Magnetic fields that are of interest for confining toroidal plasmas must have magnetic surfaces in much of the plasma volume. A magnetic field which has perfect surfaces throughout the volume of interest is said to be integrable; so the magnetic fields associated with toroidal confinement must have a neighboring integrable field. This means that the canonical coordinates of the field line Hamiltonian can always be chosen so that the Hamiltonian is a function of the canonical momentum alone plus a small perturbation. Such Hamiltonians are said to be in near-action-angle form, and standard Hamiltonian perturbation theory gives methods for locating and assessing the importance of islands and stochastic regions. Consequently, the determination of the field line Hamiltonian not only reduces the study of the structure of the field lines from a vector to a scalar problem, but it also gives a concise and complete statement of the quality of the magnetic surfaces provided near-action-angle canonical coordinates are used. If one has a priori knowledge of the shape of the magnetic surfaces or other information on the field line trajectories, this information can be easily incorporated in the choice of canonical coordinates to make the field line Hamiltonian close to the action-angle form. The method that we will use to find the field line Hamiltonian makes it close to the action-angle form by using information from a single field line trajectory.

## II. THEORETICAL BASIS

The methods that will be used to examine the structure of a given magnetic field are a generalization of magnetic coordinate techniques. Therefore, the properties of magnetic coordinates will be reviewed (Section II.a) before the more general canonical representation is discussed (Section II.b). In addition to magnetic and canonical coordinates, there are three technical points which must be dealt with. First, we must know the conditions that are required for a set of transformation equations to be analytic in order to obtain smooth transformation equations from a few field line integrations (Section II.c). Second, we must know the relations between the near-magnetic coordinate form for the Hamiltonian and the properties of magnetic islands. These relations are needed if the Hamiltonian method is to be compared with the ordinary Poincaré plot method for studying magnetic field structure (Section II.d). Third, we must develop the second-order perturbation theory that is needed to transform canonically the Hamiltonian into the appropriate near-magnetic coordinate form (Section II.e).

### a. *Magnetic Coordinates*

If the field lines of a magnetic field  $\mathbf{B}(\mathbf{x})$  lie in nested toroidal surfaces, then the magnetic field is integrable and can be described by the well-known magnetic coordinate representation

$$\mathbf{B}(\mathbf{x}) = \nabla\psi \times \nabla\theta + \nabla\varphi \times \nabla\chi(\psi). \quad (1)$$

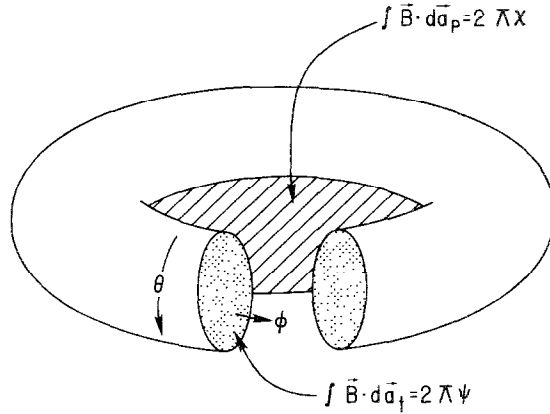


FIG. 1. Canonical coordinates. The poloidal flux outside a constant  $\chi$  surface is  $2\pi\chi$ . The toroidal magnetic flux inside a constant  $\psi$  surface is  $2\pi\psi$ . However, the constant  $\psi$  and the constant  $\chi$  surfaces need not be identical. The poloidal angle is  $\theta$  and the toroidal angle is  $\phi$ .

The physical interpretation of  $\psi$ ,  $\theta$ ,  $\phi$  and  $\chi$  is given in Fig. 1. The primary feature of magnetic coordinates is that they trivialize the problem of evaluating the trajectory of a field line. A field line trajectory obeys the relations

$$\psi = \psi_0 \quad \text{and} \quad \theta = \theta_0 + \iota(\psi) \phi \tag{2}$$

with  $\iota = d\chi/d\psi$ , the rotational transform, and with  $\psi_0$  and  $\theta_0$  constants. The trajectory relations follow from the obvious equations  $\mathbf{B} \cdot \nabla\psi = 0$  and  $\mathbf{B} \cdot \nabla(\theta - \iota\phi) = 0$ . To actually trace the field lines in ordinary space, the transformation equations  $\mathbf{x}(\psi, \theta, \phi)$  which give the spatial location of each  $\psi, \theta, \phi$  point, are required in addition to  $\chi(\psi)$ . Conversely, the dual relations of partial differentiation theory can be used to show that any two functions  $\chi(\psi)$  and  $\mathbf{x}(\psi, \theta, \phi)$  uniquely specify a magnetic field  $\mathbf{B}(\mathbf{x})$ . The dual relations are

$$\nabla\psi = \frac{1}{J} \left( \frac{\partial\mathbf{x}}{\partial\theta} \times \frac{\partial\mathbf{x}}{\partial\phi} \right) \quad \text{and} \quad \frac{\partial\mathbf{x}}{\partial\psi} = J(\nabla\theta \times \nabla\phi) \tag{3}$$

with even permutations of the  $\psi, \theta, \phi$  labels also giving valid relations.

The Jacobian  $J$  is defined by

$$J = \frac{\partial\mathbf{x}}{\partial\psi} \cdot \left( \frac{\partial\mathbf{x}}{\partial\theta} \times \frac{\partial\mathbf{x}}{\partial\phi} \right) = (\nabla\psi \times \nabla\theta) \cdot \nabla\phi. \tag{4}$$

The dual relations together with Eq. (1) imply

$$\mathbf{B} = \frac{1}{J} \left( \frac{\partial\mathbf{x}}{\partial\phi} + \iota \frac{\partial\mathbf{x}}{\partial\theta} \right) \tag{5}$$

and demonstrate that  $\mathbf{x}(\psi, \theta, \phi)$  and  $\chi(\psi)$  uniquely specify  $\mathbf{B}$ .

The magnetic coordinate functions  $\mathbf{x}(\psi, \theta, \varphi)$  and  $\chi(\psi)$ , which provide a particularly useful representation of the magnetic field, can be evaluated computationally [6, 7] for any given integrable field  $\mathbf{B}(\mathbf{x})$ . To carry out this evaluation, a field line trajectory  $\mathbf{x}(\varphi)$  is determined by integrating the differential equation

$$\frac{d\mathbf{x}}{d\varphi} = \frac{\mathbf{B}(\mathbf{x})}{\mathbf{B} \cdot \nabla\varphi} \quad (6)$$

with a definite choice of toroidal angle  $\varphi(\mathbf{x})$ . One can show that the toroidal angle of magnetic coordinates can be chosen arbitrarily, but the most convenient choice is often the azimuthal angle, which is the angle of cylindrical coordinates  $R, \varphi, Z$  (Fig. 2). Knowing  $\mathbf{x}(\varphi)$  along field lines, one can obtain  $\mathbf{x}(\psi, \theta, \varphi)$  and  $\iota(\psi)$  using the periodicity of the poloidal and toroidal directions, namely,

$$\mathbf{x}(\psi, \theta, \varphi) = \sum \mathbf{x}_{nm}(\psi) \exp[i(n\varphi - m\theta)]. \quad (7)$$

Equations (2) and (7) imply that the functional form of a field line  $\mathbf{x}(\varphi)$  must be

$$\mathbf{x}(\varphi) = \sum \mathbf{x}_{nm}(\psi) \exp[i(n - im)\varphi] \quad (8)$$

with  $\theta_0$  assumed zero, which is always possible. A Fourier decomposition of a known trajectory  $\mathbf{x}(\varphi)$  gives the  $\mathbf{x}_{nm}$  and  $\iota$  on a magnetic surface. The toroidal magnetic flux  $2\pi\psi$  associated with that surface can be determined by an area integral.

### b. Canonical Coordinates

A general magnetic field is constrained only by one condition,  $\nabla \cdot \mathbf{B} = 0$  globally, and cannot be written in magnetic coordinate form. Nevertheless, if  $\mathbf{B} \cdot \nabla\varphi$  is non-

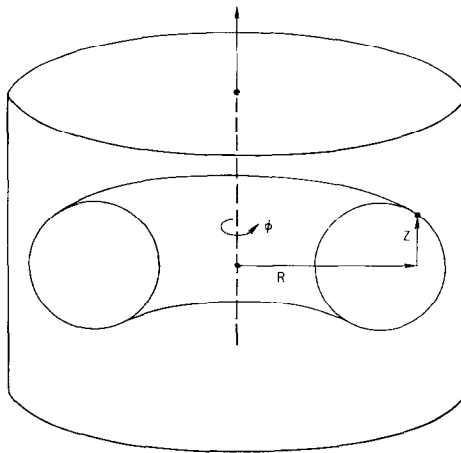


FIG. 2. The use of cylindrical coordinates for describing a toroidal configuration is illustrated.

zero, an otherwise general divergence-free field can be written in the canonical representation [5]

$$\mathbf{B} = \nabla\psi \times \nabla\theta + \nabla\varphi \times \nabla\chi(\psi, \theta, \varphi). \quad (9)$$

The magnetic coordinate representation is a special case of the canonical representation in which the poloidal flux function  $\chi$  is a function of  $\psi$  alone.

The poloidal flux function  $\chi(\psi, \theta, \varphi)$  is also the field line Hamiltonian. This can be demonstrated by using  $d\psi/d\varphi = (\nabla\psi) \cdot d\mathbf{x}/d\varphi$  and Eqs. (6) and (9) to show that

$$\frac{d\psi}{d\varphi} = -\frac{\partial\chi}{\partial\theta} \quad \text{and} \quad \frac{d\theta}{d\varphi} = \frac{\partial\chi}{\partial\psi}. \quad (10)$$

As in magnetic coordinates, the flux function  $\chi$  and the transformation equations  $\mathbf{x}(\psi, \theta, \varphi)$  uniquely specify the magnetic field. The important feature of canonical coordinates is that the structure of the magnetic field is determined by  $\chi(\psi, \theta, \varphi)$  alone. This follows from the fact that well-behaved transformations do not alter topological features of the field such as magnetic islands or stochastic regions. In practice one rarely needs to know the spatial location of a field line trajectory with as great an accuracy as one needs to know its topological structure such as the existence of nested magnetic surfaces. This means that only the magnetic Hamiltonian need be evaluated with high numerical accuracy. The magnetic Hamiltonian can be conveniently represented in Fourier series form

$$\chi = \chi_0(\psi) + \sum \chi_{nm}(\psi) \exp[i(n\varphi - m\theta)]. \quad (11)$$

The canonical coordinates of a given field  $\mathbf{B}(\mathbf{x})$  are not unique; there is the freedom of canonical transformations [8], which are a major part of the Hamiltonian theory of classical mechanics. The most useful canonical coordinates, near-magnetic coordinates, are as close as possible to magnetic coordinates in the sense that only resonant  $\chi_{nm}$  Fourier coefficients occur in the series. A Fourier coefficient is resonant if  $\iota = d\chi_0/d\psi$  satisfies  $n = im$  for a value of  $\psi$  in the region of interest. The resonant Fourier terms in near-magnetic coordinates represent magnetic islands or stochastic field line regions. These features are topological and therefore appear regardless of which coordinate system is used to describe the field.

The arbitrariness of the canonical coordinates eases the problem of evaluation. Let  $\mathbf{x}(\rho, \theta, \varphi)$  be a set of transformation equations which are arbitrary except that the Jacobian is finite;  $\theta$  and  $\varphi$  are a poloidal and a toroidal angle, respectively; and  $\rho$ , the radial coordinate, is zero along the axis of the poloidal angle. Equations for evaluating the canonical coordinates of a given field  $\mathbf{B}(\mathbf{x})$  are derived by dotting Eq. (9) with  $\nabla\varphi$  and  $\nabla\theta$  while considering  $\psi$  and  $\chi$  to be functions of  $\rho, \theta, \varphi$ . That is,  $\partial\psi/\partial\rho = J_\rho \mathbf{B} \cdot \nabla\varphi$  and  $\partial\psi/\partial\rho = J_\rho \mathbf{B} \cdot \nabla\theta$  with  $J_\rho$  the  $\rho, \theta, \varphi$  Jacobian. The dual relations of partial differentiation theory, which relate  $\nabla\theta$  and  $\nabla\varphi$  to derivatives of

the transformation equation  $\mathbf{x}(\rho, \theta, \varphi)$  (Eq. (5)), allow one to obtain the differential equations [5]

$$\frac{\partial \rho}{\partial \psi} = \frac{1}{\mathbf{B} \cdot [(\partial \mathbf{x} / \partial \rho) \times (\partial \mathbf{x} / \partial \theta)]}, \quad \frac{\partial \chi}{\partial \psi} = \frac{\mathbf{B} \cdot [(\partial \mathbf{x} / \partial \varphi) \times (\partial \mathbf{x} / \partial \rho)]}{\mathbf{B} \cdot [(\partial \mathbf{x} / \partial \rho) \times (\partial \mathbf{x} / \partial \theta)]}. \quad (12)$$

The right-hand sides of these equations are known functions of  $\rho, \theta, \varphi$ . To integrate them, one picks a value of  $\theta$  and  $\varphi$  and uses the boundary conditions, which are implied by regularity, that  $\rho$  is zero and  $\chi$  is a constant at  $\psi$  equal to zero [see Eq. (14); also note that a purely  $\varphi$ -dependent, additive term to  $\chi$  is irrelevant]. After evaluating  $\chi$  for a number of  $\theta, \varphi$  values, one can use a fast Fourier transform to obtain  $\chi$  in Fourier-decomposed form (Eq. (11)). For an analytic field the Fourier coefficients converge exponentially; so the number of  $\theta, \varphi$  values required to obtain an accurate Hamiltonian is small. In principle one should integrate  $B$  over the area enclosed by the curve  $\psi = 0$  to obtain the poloidal flux  $2\pi\chi_0(0)$ , but this constant, which is additive to  $\chi$ , is important only in time-dependent problems and will be ignored.

The magnetic fields that we wish to study are nearly integrable. This means that for a number of toroidal transits the trajectory of a field line will remain close to one surface in a set of nested toroidal surfaces. Nearly integrable fields can be studied by using a few short trajectory integrations to set up a smooth approximation to magnetic coordinate transformations equations [see Eq. (8) and the related discussion]. If these transformation equations are denoted by  $\mathbf{x}(\rho, \theta, \varphi)$ , then the procedure outlined in the discussion of Eq. (12) gives the magnetic Hamiltonian  $\chi(\psi, \theta, \varphi)$  and the canonical transformation equations  $\mathbf{x}(\psi, \theta, \varphi)$ . If the field were integrable, and if the magnetic coordinate evaluation were carried out with perfect accuracy, then  $\chi$  would be a function of  $\psi$  alone. For nearly integrable fields,  $\chi$  will not be a function of  $\psi$  alone, but the angle-dependent part of  $\chi$  will be small compared to  $\chi_0(\psi)$ . Consequently, one can use a simple perturbation analysis, although frequently of second order, to search for magnetic islands.

### c. Analyticity Conditions

The analyticity conditions for polar coordinates, such as the  $\rho$  and  $\theta$  coordinates, can be determined by defining pseudo-Cartesian coordinates  $\xi = r \cos(\theta)$  and  $\eta = r \sin(\theta)$ . The reason for defining  $\xi$  and  $\eta$  is that analyticity gives conditions near the origin of the polar coordinates. Both  $\xi$  and  $\eta$  go to zero at the origin, but the  $\theta$  coordinate does not. The reason for using the symbol  $r$ , instead of  $\rho$ , for the radial coordinate is that  $r$  will be assumed proportional to distance near the origin. The radial coordinate  $\rho$  is often taken to be a flux coordinate, which is proportional to the distance from the origin squared. Any analytic function  $f$  has a Taylor expansion in  $\xi$  and  $\eta$  near the origin. That is, for  $\xi$  and  $\eta$  sufficiently small,  $f$  can be written as

$$f = \sum f_{jk} \xi^j \eta^k = \sum f_{jk} r^{j+k} \cos(\theta)^j \sin(\theta)^k. \quad (13)$$

The function  $\cos(\theta)^j \sin(\theta)^k$  can be written as a Fourier series in  $\cos(m\theta)$  and  $\sin(m\theta)$ . This series contains values of  $m$  only in the range  $0 \leq m \leq j+k$  and only even or odd values of  $m$  depending on whether  $j+k$  is even or odd. (Throughout this paper we use the convention that the poloidal mode number  $m$  is positive.) An analytic function of position  $f$  can therefore be put in the form

$$f(r, \theta) = \sum r^m [a_m(r^2) \cos(m\theta) + b_m(r^2) \sin(m\theta)] \quad (14)$$

with the  $a_m$  and  $b_m$  analytic functions of  $r^2$ . Equation (14) will be used to obtain smooth transformation equations. The analyticity conditions for one set of polar coordinates expressed in terms of another are subtle since neither the polar angle  $\theta$  nor the radial coordinate  $r$  is an analytic function of position. For this reason it is best to use spatial coordinates that are not polar around the axis of the poloidal angle, such as the  $R, \varphi, z$  coordinates of Fig. (2).

#### d. Comparison of a Poincaré Plot with a Hamiltonian

It is important to have a method for comparing magnetic islands as seen in a conventional Poincaré plot with their representation using the magnetic Hamiltonian. The number of toroidal circuits  $N_0$  required for a field line to encircle the island  $O$ -point on the Poincaré plot gives such a comparison. This number is almost constant for field lines inside the island except for a logarithmic singularity at the island separatrix. The number  $N_0$  can be evaluated for the magnetic Hamiltonian

$$\chi = \chi_0(\psi) - \tilde{\chi} \cos(n\varphi - m\theta), \quad (15)$$

which has a magnetic island about the surface  $\psi_0$  on which  $i = n/m$  with  $i = d\chi/d\psi$ . If we assume that  $i' = di/d\psi$  and  $\tilde{\chi}$  are positive, then the  $O$ -point of the island is at  $\psi = \psi_0$  and  $\theta = \theta_0$  with  $\theta_0 = n\varphi_0/m$ . Expanding the Hamiltonian about  $\psi_0, \theta_0$  and ignoring an additive constant,

$$\chi \approx \frac{n}{m} (\psi - \psi_0) + \frac{1}{2} i' (\psi - \psi_0)^2 + \frac{1}{2} \tilde{\chi} m^2 (\theta - \theta_0)^2. \quad (16)$$

Using Hamilton's equations (Eq. (10)), one can easily show that the trajectories are

$$\psi = \psi_0 + \psi_1 \exp(i\varphi/N_0) \quad \text{and} \quad \theta = \theta_0 + iN_0 i' \psi_1 \exp(i\varphi/N_0) \quad (17)$$

with  $\psi_1$  a constant and

$$N_0 = \frac{1}{m(i'\tilde{\chi})^{1/2}}. \quad (18)$$

Each time  $\varphi$  advances by  $2\pi N_0$ , the Poincaré plot of a field line shows the line encircling the  $O$ -point.

e. *The Canonical Perturbation Theory*

The Fourier decomposition of the magnetic Hamiltonian (Eq. (11)) frequently contains large, nonresonant, Fourier terms. Perturbation theory can be used to find a canonical transformation that removes these nonresonant terms, but there is a correction to the resonant Fourier terms, which create islands, that is second order in the nonresonant terms. Consequently, an accurate study of the islands frequently necessitates the use of second-order perturbation theory. Any Hamiltonian can be written as  $\chi = \chi_0(\psi) + \tilde{\chi}(\psi, \theta, \varphi) + \hat{\chi}(\psi, \theta, \varphi)$  with  $\tilde{\chi}$  containing only nonresonant Fourier terms and  $\hat{\chi}$  containing only resonant Fourier terms. Let  $\chi$  be a function of a parameter  $\varepsilon$  as well as  $\psi, \theta, \varphi$ , then one can canonically transform away the nonresonant Fourier terms by integrating the equations [9]

$$\partial\chi_0(\psi, \varepsilon)/\partial\varepsilon = \partial s/\partial\varphi + \iota\partial s/\partial\theta + \tilde{\chi} - \varepsilon\sigma \quad (19)$$

$$\partial\tilde{\chi}(\psi, \theta, \varphi, \varepsilon)/\partial\varepsilon = [\tilde{\chi}, s] - \sigma \quad (20)$$

$$\partial\hat{\chi}(\psi, \theta, \varphi, \varepsilon)/\partial\varepsilon = [\hat{\chi}, s] + \sigma \quad (21)$$

with  $s$  and  $\sigma$  functions of  $\psi, \theta, \varphi, \varepsilon$  which are chosen so that  $\tilde{\chi}$  remains nonresonant and  $\hat{\chi}$  remains resonant,  $\iota = \partial\chi_0/\partial\psi$ , and  $[\cdot, \cdot]$  is the Poisson bracket. That is,

$$[\tilde{\chi}, s] = (\partial\tilde{\chi}/\partial\psi)(\partial s/\partial\theta) - (\partial\tilde{\chi}/\partial\theta)(\partial s/\partial\psi). \quad (20)$$

At  $\varepsilon=0$  one lets  $\chi_0, \tilde{\chi}$ , and  $\hat{\chi}$  equal the given functions; at  $\varepsilon=1$  the exact Hamiltonian has no resonant terms and  $\chi = \chi_0 + \hat{\chi}$ . Although the exact removal of the nonresonant Fourier terms using Eqs. (19) to (22) can be very useful, here we consider only a second-order analysis. We assume the  $\tilde{\chi}$  terms are sufficiently large that second-order terms due to  $\tilde{\chi}$  are of the same magnitude as  $\hat{\chi}$ . By a second-order term we mean the solutions to the differential equations (19)–(21) are Taylor expanded in  $\varepsilon$  to order  $\varepsilon^2$  and the second-order Taylor expansion is assumed valid at  $\varepsilon=1$ . One can then show that at  $\varepsilon=1$

$$\chi_0(\psi) = \chi_{00}(\psi) + [\tilde{\chi}_0, s_0]_a/2 \quad (23)$$

$$\hat{\chi}(\psi, \theta, \varphi) = \hat{\chi}_0 + [\tilde{\chi}_0, s_0]_r \quad (24)$$

with the subscript “a” implying an average over  $\theta, \varphi$  and “r” implying that only resonant Fourier terms are retained. The final subscript “0” in  $\chi_{00}, \tilde{\chi}_0$  and  $\hat{\chi}_0$  implies that the initial,  $\varepsilon=0$ , expression is used. The function  $s_0$ , which is a so-called infinitesimal generating function, is given by

$$\partial s_0/\partial\varphi + \iota_0 \partial s_0/\partial\theta + \tilde{\chi}_0 = 0. \quad (25)$$

A single nonresonant Fourier term cannot produce a resonant Fourier term, but such a term can modify the transform  $\iota$  and therefore move the location of the resonance. That is, if  $\tilde{\chi}_0 = \chi_1(\psi) \cos(n\varphi - m\theta)$ , then

$$[\chi_0, s_0]_a = [m/(n - \iota_0 m)] \chi_1' \chi_1 + [m\chi_1/(n - \iota_0 m)]^2 \iota_0'/2. \quad (26)$$



The first term in this expression is the so-called stellarator expansion term for the poloidal flux function [10]. The more important case is one in which there are two, or more, nonresonant Fourier terms. The general case can be treated by summing up the second-order interaction of each nonresonant term with itself (Eq. (26)), and its beats with every other nonresonant term, with each pair of terms counted once. Consider  $\tilde{\chi}$  of the form  $\tilde{\chi} = \chi_1(\psi) \cos(n_1\varphi - m_1\theta) + \chi_2(\psi) \cos(n_2\varphi - m_2\theta)$ , then

$$[\tilde{\chi}, s_0]_r = a_1 \cos[(n_1 + n_2)\varphi - (m_1 + m_2)\theta] + a_2 \cos[(n_1 - n_2)\varphi - (m_1 - m_2)\theta]. \quad (27)$$

The  $a_1$ , or upshift, term is normally more important than the downshift, or  $a_2$ , term. We therefore only give the expression for  $a_1$ ,

$$a_1 = -\frac{m_1 m_2 \chi_1 \chi_2' \iota_0'}{2} \left[ \frac{1}{(n_1 - \iota_0 m_1)^2} + \frac{1}{(n_2 - \iota_0 m_2)^2} \right]. \quad (26)$$

At the resonance  $\iota_0 = (n_1 + n_2)/(m_1 + m_2)$ , the terms  $(n_1 - \iota_0 m_1)^2$  and  $(n_2 - \iota_0 m_2)^2$  are equal.

### III. NUMERICAL IMPLEMENTATION

To give a simple illustration of the Hamiltonian method, we will study the vacuum magnetic field of a cylinder. This field can be expressed analytically while retaining all the features of interest of the toroidal equivalent. The general vacuum field in a cylinder with coordinates  $r, \alpha, z$  that has no internal currents is

$$\mathbf{B} = B_0 \hat{\mathbf{z}} + \nabla \left[ \sum (R/n) b_{nm} I_m(nr/R) \cos(n\varphi - m\alpha) \right] \quad (29)$$

plus a similar sine series. The  $I_m$  are the modified Bessel functions,  $2\pi R$  is the periodicity distance along the axis of the cylinder, and  $\varphi = z/R$  is equivalent to the toroidal angle (Fig. 3). The position vector in cylindrical coordinates,

$$\mathbf{x} = r\hat{\mathbf{r}}(\alpha) + z\hat{\mathbf{z}} \quad (30)$$

with  $d\mathbf{r}/d\alpha = \hat{\mathbf{a}}$ , can be used to obtain the field line equations (see Eq. (6)),

$$dr/d\varphi = RB_r/B_z \quad \text{and} \quad d\alpha/d\varphi = RB_\alpha/(rB_z). \quad (31)$$

The field which will be studied has only two Fourier components,  $b_{12}/B_0 = 1.68$  and  $b_{16}/B_0 = 900$ . The constant field  $B_0$  is taken to have unit strength and the periodicity distance  $R$  is taken to have unit length. The field will be investigated in the region  $r < 0.4$ ; so the modified Bessel functions are small,  $I_2 < 2 \times 10^{-2}$  and  $I_6 < 9 \times 10^{-8}$ . Despite the large value for  $b_{16}$ , the field is essentially that of an  $m = 2$  stellarator. The rotational transform varies from  $\iota \approx 0.225$  at the axis and would

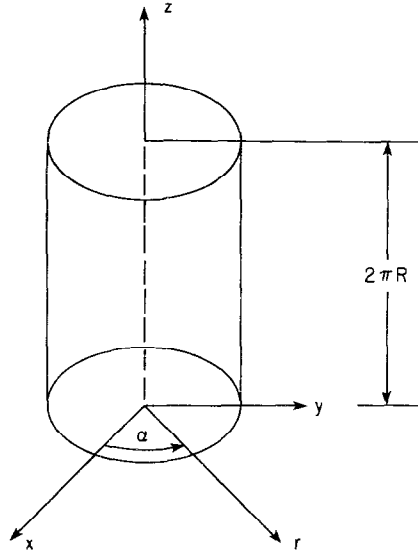


FIG. 3. The cylindrical coordinates used in the computation of the model field.

increase to  $\iota = 0.5$  at the separatrix (Fig. 4). A small magnetic island chain is driven around the  $\iota = 0.25$  surface due to the beating of the  $m = 2$  and  $m = 6$  Fourier terms (Fig. 5).

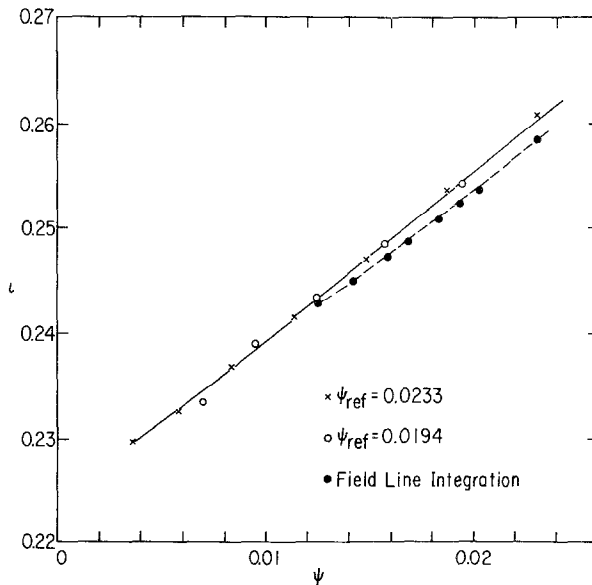


FIG. 4. The rotational transform  $\iota$  versus the toroidal flux function  $\psi$ . The dashed line is obtained from a field line integration. The solid line is  $d\chi_{00}/d\psi$ . The difference between the two curves is the contribution to the transform of the  $\chi_{12}$  Fourier term in the Hamiltonian.

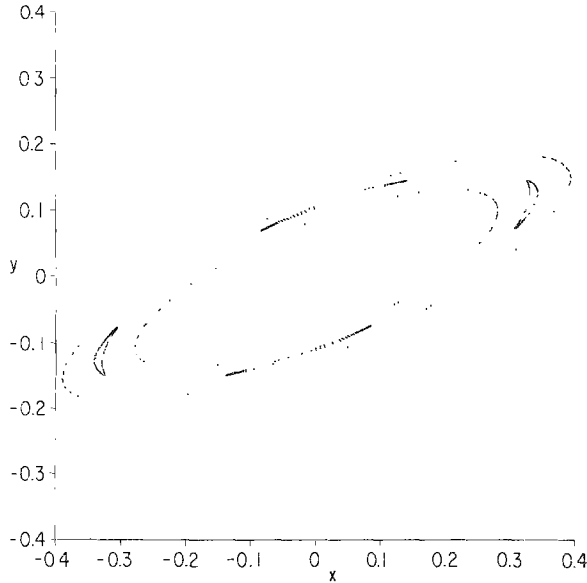


FIG. 5. Ordinary space Poincaré plot. The intersections of three field lines with a constant  $\varphi$  plane are plotted. The four islands on the plot are part of the trajectory of a single line. Since the resonance is a second harmonic  $2/8$ , not a first harmonic  $1/4$ , resonance, there are two unconnected, but interweaving, sets of islands. A more complete Poincaré plot would require another field line trajectory to show that there is an additional set of four islands about the same resonant surface with one of the additional islands in each of the four empty spaces between the illustrated islands.

The magnetic field which has been defined can be studied in two ways: by the traditional Poincaré plot (for example, on the  $\varphi = 0, 2\pi, \dots$  surfaces) and by the Hamiltonian method. The Poincaré method consists of a straightforward integration of Eq. (21) for the field lines using a 4th-order Runge-Kutta scheme at equal  $\varphi$  intervals. This is the method of construction of Fig. 5. The Poincaré plot of the outermost field line, which has a transform of  $\iota = 0.2524$ , appears to be forming a smooth magnetic surface; so the method outlined in the discussion of Eq. (8) can be utilized to evaluate magnetic coordinates for this surface. To simplify the imposition of the analyticity constraints, the field line trajectory is recorded in Cartesian coordinates  $x = r \cos(\alpha)$  and  $y = r \sin(\alpha)$  (see Fig. 3). In other words, the field line integration determines  $x(\varphi)$  and  $y(\varphi)$  which are Fourier decomposed to obtain the Fourier coefficients of

$$x(\theta, \varphi) = \sum \bar{x}_{nm} \cos(n\varphi - m\theta) \quad \text{and} \quad y(\theta, \varphi) = \sum \bar{y}_{nm} \sin(n\varphi - m\theta). \quad (32)$$

Due to the form of the field, only cosine terms are needed to describe the  $x$  coordinate and sine terms to describe the  $y$  coordinate. Most stellarator fields of practical interest have the analogous property for the major radius  $R$  and the vertical

TABLE I  
Fourier Components of the Position Coordinates  
of the Magnetic Field Line

$n$	$m$	$\bar{x}_{nm}$	$\bar{y}_{nm}$
0	-1	0.23838	0.23838
1	1	0.14206	0.14206

coordinate  $z$  (Fig. 2). The Fourier decomposition was carried out using field line data from 256 equivalent toroidal circuits using a fast Fourier transform and a Gaussian window function [6, 7]. At the same time, we calculate the toroidal flux  $2\pi\psi$  from  $\int \mathbf{B} \cdot d\mathbf{a}$  (Fig. 1). Only two Fourier coefficients were used to represent each of the two coordinates,  $x$  and  $y$ . These are given in Table I.

The surface reconstructed from these Fourier coefficients is outlined by crosses in Fig. 6. The dotted curve, by comparison, shows the Poincaré plot of the outermost field line of Fig. 5. The initial transformation equations  $\mathbf{x}(\rho, \theta, \varphi)$  are set by the Fourier components of Table I. The Fourier components of  $\mathbf{x}(\rho, \theta, \varphi)$  are

$$x_{nm}(\rho) = \bar{x}_{nm}\rho^{m/2} \quad \text{and} \quad y_{nm}(\rho) = \bar{y}_{nm}\rho^{m/2}, \quad (33)$$

with  $\rho$ , the radial coordinate, having the value unity at the reference surface.

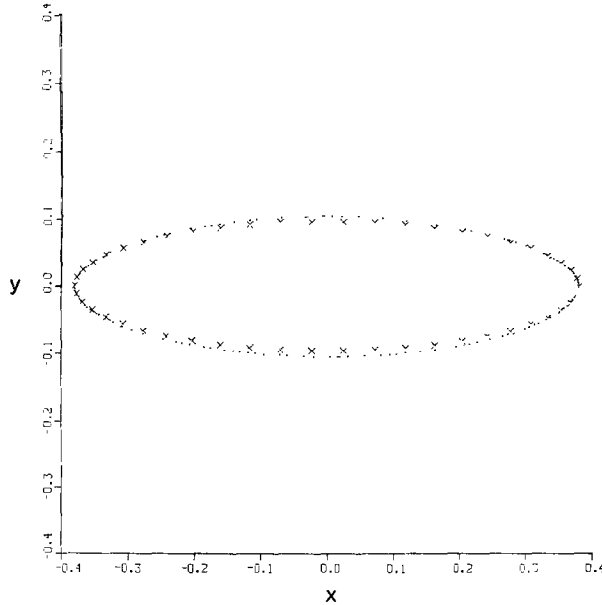


FIG. 6. Initial transformation equations. The  $\times$  symbols lie on the surface obtained from the Fourier components of the coordinates  $x$  and  $y$  that are given in Table I. The dots form a Poincaré plot of the field line with transform  $\iota = 0.2524$ . The largest Fourier terms in the transformation equations to magnetic coordinates for this field line were used to obtain Table I.

The magnetic Hamiltonian  $\chi(\psi, \theta, \varphi)$  is obtained by integrating the differential equations of Eq. (12). These differential equations are integrated as ordinary differential equations in  $\psi$  on a grid of 64 equally spaced values of  $\theta$  and 16 equally spaced values of  $\varphi$ . The value of  $\chi(\psi, \theta, \varphi)$  is recorded at 10 evenly spaced  $\sqrt{\psi}$  values for each value of  $\theta$  and  $\varphi$ . A fast Fourier transform then gives the Fourier series for  $\chi$  on each  $\psi$  surface. The behavior of the most important Fourier components,  $\chi_{12}(\psi)$ ,  $\chi_{16}(\psi)$  and  $\chi_{28}(\psi)$ , are given in Fig. 7. The exponential convergence of the Fourier series for  $\chi$  is illustrated in Fig. 8, which gives the amplitudes of the  $n=2$  Fourier terms at  $\psi = 1.78 \times 10^{-2}$  for various values of  $m$ . The symmetry of the magnetic field implies that only multiples of  $m=4$  can appear.

There are two curves in Fig. 4 for the rotational transform  $i(\psi)$ . The dashed curve is derived from a field line integration with the toroidal flux  $2\pi\psi$  determined by integrating  $\mathbf{B} \cdot d\mathbf{a}$  over the cross section of the apparent magnetic surface. The full curve is  $d\chi_{00}/d\psi$ , the derivative of the  $n=0$ ,  $m=0$  Fourier component of the Hamiltonian. This must be corrected for the contribution of the nonresonant terms, of which  $\chi_{12}$  is the most dominant, to obtain the rotational transform of the field.

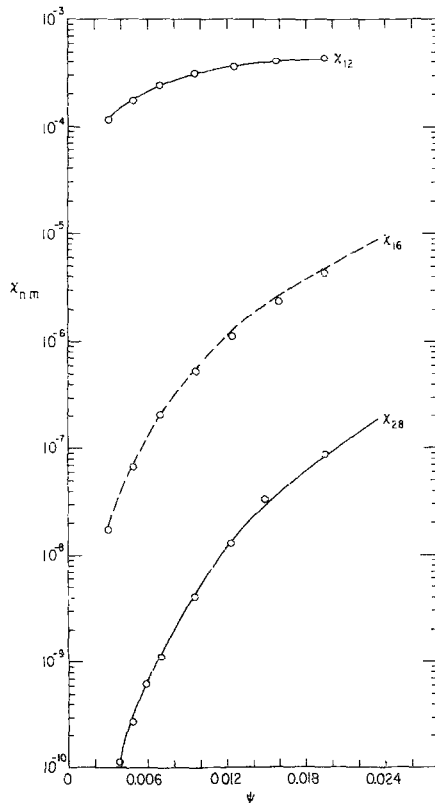


FIG. 7. The  $\psi$  dependence of the three most important Fourier components of the Hamiltonian,  $\chi_{12}$ ,  $\chi_{16}$ , and  $\chi_{28}$ , are illustrated.

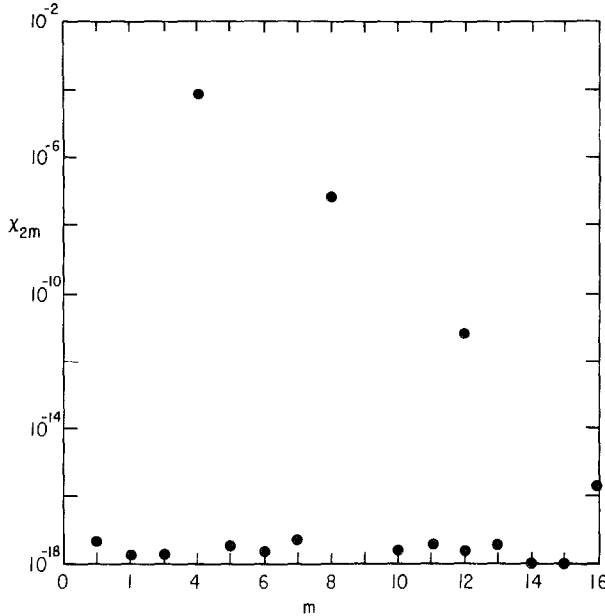


FIG. 8. The poloidal mode number dependence of the  $n=2$  Fourier terms in the Hamiltonian is illustrated. There is a clear exponential convergence at high  $m$  as expected for an analytic field. Only multiples of  $m=4$  are present due to the symmetry of the field.

This correction can be made using Eqs. (23) and (26) and we have therefore  $\iota = d\chi_{00}/d\psi + \Delta\iota$ . If we ignore the second term in  $\Delta\iota$  due to the shear  $d\iota/d\psi = 1.56$ , then Eqs. (23) and (26) imply

$$\Delta\iota = \frac{m}{n - im} \left[ \frac{d^2\chi_{12}}{d\psi^2} \chi_{12} + \left( \frac{d\chi_{12}}{d\psi} \right)^2 \right] / 2. \quad (34)$$

Computed values for  $d\chi_{12}/d\psi$  and  $d^2\chi_{12}/d\psi^2$  at the resonant surface,  $\psi = 1.78 \times 10^{-2}$ , give  $\Delta\iota = -0.0018$ . The displacement in  $\psi$  for the full curve from the dotted curve is therefore  $\Delta\psi = \Delta\iota/(d\chi/d\psi) = -0.0011$ , which is in full agreement with measurements from Fig. 4.

To study the island structure at  $\iota = 2/8$ , which is  $\psi = 1.78 \times 10^{-2}$ , the amplitudes of the potentially resonant Fourier terms in the Hamiltonian are required. The important Fourier terms in the Hamiltonian are given in Table II.

The resonant  $n=2$ ,  $m=8$  term is driven not only by the direct  $\chi_{28}$  term in the Hamiltonian, but also by the coupling of  $\chi_{12}$  and  $\chi_{16}$ , and  $\chi_{04}$  and  $\chi_{24}$  terms. With the use of Eq. (28) and associated equations, we find  $a_1 = 1.089 \times 10^{-7}$  for the coupling of  $\chi_{12}$  and  $\chi_{16}$  and  $a_1 = -0.261 \times 10^{-7}$  for the coupling of  $\chi_{04}$  and  $\chi_{24}$ . Therefore the total resonant term  $\hat{\chi}_{28} = \chi_{28} + 1.089 \times 10^{-7} - 0.261 \times 10^{-7} = 1.369 \times 10^{-7}$ . This value together with  $d\iota/d\psi = 1.56$  implies that it would take 276 circuits of the torus for a field line to encircle the island magnetic axis (Eq. (18)). If

TABLE II  
Fourier Components of the Hamiltonian

$n$	$m$	$\chi_{nm}$
0	0	$4.244 \times 10^{-3}$
0	4	$1.240 \times 10^{-5}$
2	4	$8.777 \times 10^{-5}$
1	2	$-4.246 \times 10^{-4}$
1	6	$3.563 \times 10^{-6}$
2	8	$5.400 \times 10^{-8}$

the island is wide enough, the number of toroidal circuits can be obtained by counting the number of dots on an ordinary Poincaré plot required to encircle the island axis. As the island width decreases, the Poincaré plot method becomes increasingly impractical, but in our case it is still feasible. The number of toroidal transits that was required to encircle the island magnetic axis was 280 on the Poincaré plot. This corresponds to a Hamiltonian perturbation  $\hat{\chi}_{28}$  of  $1.33 \times 10^{-7}$ , which is in excellent agreement with the calculated  $\hat{\chi}_{28} = 1.369 \times 10^{-7}$ .

One can, of course, check the formula for the number of toroidal circuits required to encircle an island axis by an explicit integration of the Hamiltonian. We take

$$\chi = \chi_0 + \hat{\chi}_{28} \cos(2\varphi - 8\theta) \quad \text{with } d\chi_0/d\psi = 1/4 + (\psi - \psi_0) i', \quad (35)$$

$i' = 1.56$ , and  $\psi_0 = .0178$ . The  $\psi$  dependence of  $\hat{\chi}_{28}$  is approximated by  $\psi^{m/2}$  near the resonant surface. The number of points on the Poincaré plot which is required to encircle the island axis implies that it takes 276 toroidal circuits (Fig. 9), which is in agreement with Eq. (18). An approximate island width may be directly deduced from Fig. 9. The well-known formula of Hamiltonian theory for the half-width of an island is

$$\Delta\psi = (4\chi_{nm}/i')^{1/2}. \quad (36)$$

Using  $\hat{\chi}_{28} = 1.37 \times 10^{-7}$  and  $i' = 1.56$ , we would expect  $2\Delta\psi/\psi = 0.06$ , which is roughly substantiated by Fig. 9. A more delicate test of the Hamiltonian formalism is the transformation of Fig. 9 into ordinary space using the transformation equations  $\mathbf{x}(\psi, \theta, \varphi)$ . The result of this transformation is given in Fig. 10, which should be compared to Fig. 5.

#### IV. SUMMARY

Although the Hamiltonian procedure for studying magnetic field line trajectories may appear formal, it does provide a relatively simple and compact description of complicated magnetic fields. There are two parts to the Hamiltonian analysis of a

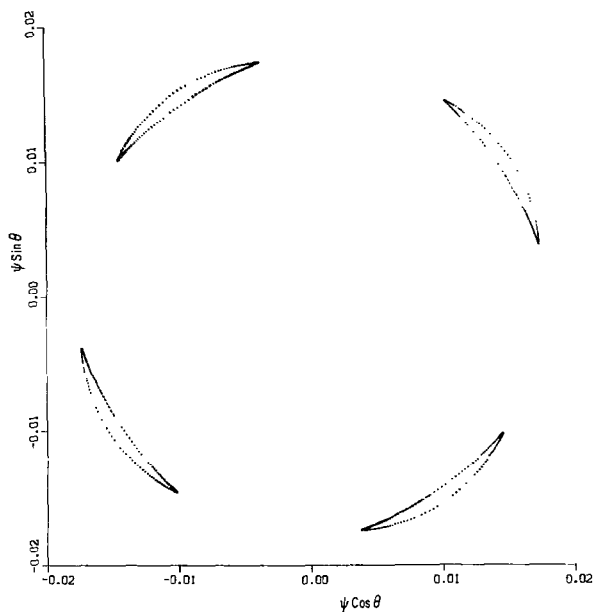


FIG. 9. Canonical coordinate space Poincaré plot. The intersection of a single field line with the constant  $\varphi$  plane is plotted by integrating the field line Hamiltonian of Eq. (10).

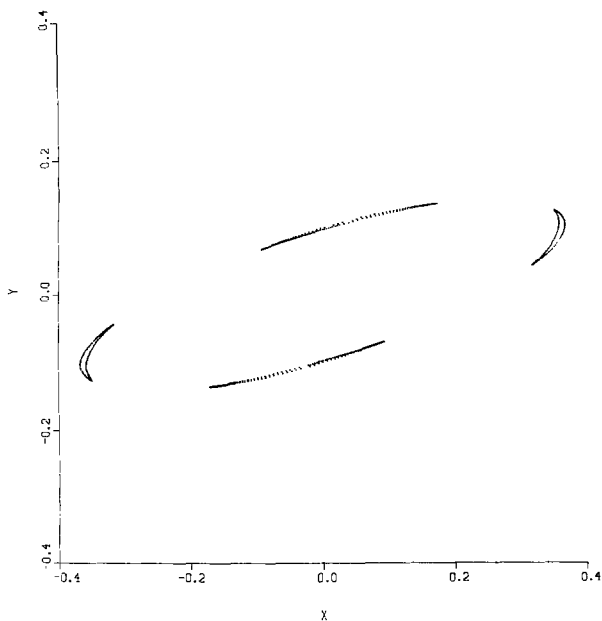


FIG. 10. Transformed Poincaré plot. The Poincaré plot of Fig. 9 is plotted in ordinary space using the transformation equations  $x(\psi, \theta, \varphi)$ . This plot should be compared with the equivalent islands of Fig. 5.



field. First, one must find the Hamiltonian  $\chi(\psi, \theta, \varphi)$  and the transformation equations  $\mathbf{x}(\psi, \theta, \varphi)$  from the canonical coordinates to ordinary space. This first part of the analysis, which is essentially finding the vector potential of the magnetic field, is carried out by integrating a pair of ordinary differential equations on a mesh of  $\theta, \varphi$  values and then Fourier decomposing in  $\theta$  and  $\varphi$  to obtain the Hamiltonian and the transformation equations in Fourier series form. The second part of the analysis is the evaluation of the field line trajectories in the canonical coordinate space. Frequently, one can obtain the Hamiltonian in a form which is close to magnetic, or action-angle, coordinates, which means  $\chi$  is a function of  $\psi$  alone plus a small perturbation. When the Hamiltonian is close to magnetic coordinate form, one can generally obtain the desired information on the field line trajectories without integrations by using canonical perturbation theory, which frequently must be a second-order theory. The use of Hamiltonian methods does allow one to remove all the Fourier terms in the Hamiltonian that depend on the toroidal and poloidal angles  $\varphi$  and  $\theta$  unless the angle-dependent terms are resonant. It is the resonant terms in the Hamiltonian that are responsible for magnetic islands and stochastic regions. The use of canonical coordinates that have only resonant angle-dependent terms in the Hamiltonian provides the simplest and most compact description of the structure of a magnetic field.

The numerical example of the study of a magnetic field by Hamiltonian methods was based on a simple analytic field. Of course the Hamiltonian, even for an analytic field, must be determined numerically; so the choice of an analytic field was made only for clarity. The example was atypical and more difficult than typical fields of physical interest in two respects. The rotational transform per period,  $\iota \approx 0.25$ , was extremely large; so the magnetic surfaces were very noncircular. The shear  $di/d\psi$ , with  $2\pi\psi$  the toroidal flux, was very small, which made the small contribution of the nonresonant terms to the transform far more important than would typically be the case. The example also used a high poloidal mode number,  $m = 8$ , island since the higher the mode number, the more difficult it is to obtain the correct width. This feature arises from the Fourier terms in an analytic Hamiltonian having a typical scaling of  $\psi^{m/2}$ . This feature is also present in ordinary space integrations of field lines; it is just not explicit as it is in the Hamiltonian method. The  $\psi^{m/2}$  typical scaling is closely related to the exponential convergence of the Fourier series of an analytic Hamiltonian. The most sensitive comparison of the field line integration in real space and the Hamiltonian solved by perturbation theory is the number of toroidal circuits it takes a field line to encircle the axis of the island. The two methods differed on this number by less than 2%.

This paper implemented for the first time a general method for finding the Hamiltonian of a given magnetic field. Although subtle, the method is simple and does allow one to utilize information that one already has on the field lines to ease the field line integrations. Indeed, the use of low-order Hamiltonian perturbation theory often eliminates the need for any numerical integrations to determine the field line trajectories and thereby gives an extremely efficient field line following package in a more general code.

## ACKNOWLEDGMENTS

One of us (G. K. P.) dedicates her work here to Keith V. Roberts, her longtime guide, friend, and philosopher, who introduced her to computational physics and taught her that no problem was too big to tackle on the computer. This work was supported by the U. S. DOE under Contract DE-AC02-76-CH0-3073.

## REFERENCES

1. L. SPITZER, JR., Princeton Project Matterhorn Report PM-3-3, NYO-995 (1951).
2. D. W. KERST, *J. Nucl. Energy C* **4**, 253 (1962).
3. M. N. ROSENBLUTH, R. Z. SAGDEEV, J. B. TAYLOR, AND G. M. ZAVLAVSKI, *Nucl. Fusion* **6**, 297 (1966).
4. H. GRAD, *Phys. Fluids* **10**, 137 (1967).
5. A. H. BOOZER, *Phys. Fluids* **26**, 1288 (1983).
6. A. H. BOOZER, *Phys. Fluids* **25**, 520 (1982).
7. G. KUO-PETRAVIC, A. H. BOOZER, J. A. ROME, AND R. H. FOWLER, *J. Comput. Phys.* **51**, 261 (1983); G. KUO-PETRAVIC, *Comput. Phys. Commun.* **33**, 353 (1984).
8. A. H. BOOZER, Princeton Plasma Physics Laboratory Report PPPL-2094R (1984).
9. A. H. BOOZER, Princeton Plasma Physics Laboratory Report PPPI-2209 (1985).
10. J. L. JOHNSON AND J. M. GREENE, *Phys. Fluids* **4**, 875 (1961).